*ICES Journal of Marine Science*, 2024, Vol. 0, Issue 0, 1–13
https://doi.org/10.1093/icesjms/fsae129
**Received:** 1 March 2024; **revised:** 21 August 2024; **accepted:** 25 August 2024
**Original Article**



# Vertical distribution of mesopelagic fishes deepens during marine heatwave in the California Current

**Ilysa S. Iglesias [1,2,*], Jerome Fiechter [1], Jarrod A. Santora [2,3], John C. Field [2]**

[1]Department of Ocean Sciences, University of California Santa Cruz, Santa Cruz, CA 95064, United States
[2]Fisheries Ecology Division, Southwest Fisheries Science Center, National Marine Fisheries Service, NOAA, Santa Cruz, CA 95060, United States
[3]Department of Applied Mathematics, University of California Santa Cruz, Santa Cruz, CA 95064, United States
*Corresponding author. Deparment of Ocean Sciences, University of California Santa Cruz, Santa Cruz, CA 95064, United States. E-mail: iiglesia@ucsc.edu

## Abstract

Marine heatwaves can impact the distribution and abundance of epipelagic organisms, but their effect on deep pelagic communities is unclear. Using fisheries acoustics data collected in the Central California current from 2013 to 2018, we found that during the warmest years of a large marine heatwave (2015–2016), the estimated center of mass depth of mesopelagic fishes deepened by up to 100 m compared to preheatwave conditions. Using a generalized additive model, we evaluated which biophysical factors may have driven these changes and found that light, dynamic height anomaly, and acoustic backscatter explained 81% of the variability in depth. We attribute the vertical shift by mesopelagic fishes into deeper waters to heatwave-driven compression of upwelling habitat that indirectly increased the amount of light reaching mesopelagic depths. Our results suggest that mesopelagic fishes are interconnected with, and thus sensitive to changes in near-surface oceanographic conditions, which could lead to cascading effects on vertical carbon export and the availability of mesopelagic fishes as prey for top predators under future climate conditions.

*Keywords:* acoustics; twilight zone; marine heatwave; mesopelagic fish; mesopelagic–epipelagic coupling

## Introduction

Mesopelagic fishes represent the greatest biomass of vertebrates on Earth, with estimates exceeding that of all global annual commercial fish landings (Irigoien et al. 2014, FAO, 2022). Mesopelagic communities contribute to global carbon export and are important prey for economically valuable and protected species such as swordfish *Xiphias gladius*, albacore *Thunnus alalunga*, and marine mammals (Brodeur and Yamamura 2005, Iglesias et al. 2023). Although the mesopelagic zone is defined as the depths of 200–1000 m, many organisms inhabiting mesopelagic depths are connected to surface processes through vertical movements into surface waters to feed. This interconnection means mesopelagic organisms are affected by anthropogenic activities that impact epipelagic habitats, such as habitat alteration, climate change, and fisheries exploitation (Martin et al. 2020, Bisson et al. 2023). Despite increasing ocean surface temperatures (IPCC 2019) and expanding oxygen minimum zones (Breitburg et al. 2018), the long-term indirect effects of climate change on mesopelagic communities are poorly understood, but predicted to increase shoaling of the deep-scattering layer (DSL) by 2100 (Proud et al. 2017), expand mesopelagic habitat (Netburn and Koslow 2015), or shift mesopelagic fishes poleward (Liu et al. 2023). Our study is the first to document changes in the vertical distribution of the mesopelagic community in response to a large heatwave event and as such, advances the identification of important current and future environmental drivers shaping mesopelagic habitat.

The largest recorded marine heatwave event to date in the northeast Pacific began in the California Current Ecosystem (hereafter CCE) as a result of increased sea level pressure in the North Pacific in 2013 (Bond et al. 2015) and eventually led to anomalous, surface intensified warm water along the US west coast, which persisted for several years (Di Lorenzo and Mantua 2016). Although the heatwave was observed in various locations and intensities between ~2014 and 2016 (Leising et al. 2015, Mcclatchie et al. 2016, Wells et al. 2017), increased temperatures in the central California Current region (where our study takes place), were not observed until late summer of 2014, and were most severe during 2015–2016 (Gentemann et al. 2017). During this time, increased sea surface temperatures led to extensive ecological change in the epipelagic community (Cavole et al. 2016), but it is less clear how this heatwave event impacted the mesopelagic community.

In the southern CCE, the abundance of larval mesopelagic fishes with northern, cold-water affinities declined, while those with warm-water affinities increased (Nielsen et al. 2021, Thompson et al. 2022). However, the extent to which these responses reflect actual changes in abundance or distribution of the adult spawners, relative to changes in either spawning intensity or the advection patterns of larval mesopelagic fishes, is uncertain. Mid-water trawl data collected at night at 30 m headrope depth along the California Coast for adult Myctophids (family Myctophidae), a dominant family of mesopelagic fishes in the California Current (Davison et al. 2015b), suggest declines in 2015, though not below mean levels (Sakuma et al. 2016). In the northern California Current (Oregon and Washington), Brodeur et al. (2019) found that the response of myctophids to the heatwave was species specific, with both increases and decreases observed during this period. However, the surveys upon which these studies are based were not designed to specifically monitor mesopelagic

populations, as trawls were conducted at 30 m headrope depth at night, and thus inadequately sample mesopelagic depths and did not allow for an evaluation in changes in the depth of mesopelagic communities during this time.

DSLs, so called because of their appearance when detected using active acoustics in deep water (Dietz 1962), are dynamic in space and time, and responsive to variable oceanographic conditions (Boswell et al. 2020). Quantifying changes in the vertical distribution of mesopelagic fishes is challenging via conventional trawl methods due to increased depths, variable diel vertical migration patterns (Catul et al. 2011), and net avoidance (Kaartvedt et al. 2012). Fisheries acoustics provide an alternative means of sampling mesopelagic fish with high spatial and temporal resolution but are biased toward gas-bearing organisms. The global estimate of mesopelagic fish biomass, previously estimated from trawl data, for example, was revised upward by an order of magnitude following an acoustic estimate (Irigoien et al. 2014). Acoustic surveys of the DSL have revealed the importance of numerous physical oceanographic conditions on DSL depth such as light (Benoit-Bird et al. 2009, Røstad et al. 2016, Aksnes et al. 2017, Boswell et al. 2020), oxygen (Bertrand et al. 1999, Netburn and Koslow 2015, Klevjer et al. 2016), temperature (Fennell and Rose 2015, Sutton et al. 2017), and thermocline depth (Peña et al. 2014, D'Elia et al. 2016). However, it is less clear how the vertical distribution of mesopelagic fishes may be affected by a large-scale marine heatwave, when many of these environmental variables undergo simultaneous, and possibly compounding, changes.

To understand the potential impacts of future oceanographic variability on mesopelagic communities, there is a need to first quantify the response of mesopelagic fishes to present conditions, especially those associated with anomalous warming events, which are predicted to increase with climate change (Di Lorenzo and Mantua 2016, Frölicher et al. 2018). In this study, we utilize a dataset of continuous active sonar data collected in the late spring of 2013–2018 within the CCE to test the hypothesis that the large marine heatwave of 2015–2016 impacted the vertical distribution of mesopelagic fish. Using *in situ* hydrographic data and remotely sensed observations, we also quantify relationships between environmental variables and the depth of mesopelagic fishes to explain how oceanographic conditions in the upper ocean could indirectly shape the vertical distribution of deep pelagic communities below.

## Methods

### Study area and survey data

The Rockfish Recruitment and Ecosystem Assessment Survey (RREAS), conducted by the Southwest Fisheries Science Center of the National Marine Fisheries Service, is an annual, late spring (i.e. May–June) survey that began in 1983 to monitor recruitment strength of rockfish and other groundfish in the CCE (Field et al. 2021, Santora et al. 2021). Continuous, multifrequency measurements of acoustic backscatter have been collected by the RREAS since 2000, although unprocessed data from 2000 to 2010 are no longer available. Our study focuses on 2013–2018 to demonstrate the impacts of the intense marine heatwave that affected the US west coast in relation to conditions preceding (2013 and 2014), during (2015 and 2016), and following (2017 and 2018) the heatwave. Acoustics data were collected from two research vessels, the R/V *Ocean Starr* (2013–2015), and the NOAA Ship *Reuben Lasker* (2016–2018) with a Simrad EK60 echosounder (Kongsberg). The geographic scope was restricted to the "core" region of the survey (36.45–38.33°N) to ensure comparable sampling coverage between years (Fig. 1). Data from 2019 were omitted due to irregularities in acoustic sampling and in 2020 due to survey cancellation during the COVID-19 pandemic. Although four dedicated acoustic transects were opportunistically sampled, most acoustic data used in this analysis were collected while in transit between predetermined trawl or CTD stations.

### Acoustic data collection and selection

Echosounder calibrations were conducted before and/or after each survey, using a 38.1 tungsten carbide calibration sphere (Foote et al. 1987, Demer et al. 2015). Underway, 38 kHz echosounder data were collected from the hull ~3.3 m (R/V *Ocean Starr)* or centreboard ~7 m (*Reuben Lasker)*, with a pulse duration of 1.024 ms and transmitted power of 2000 W, recorded to a max range of 750 m and a variable ping rate (set to maximum). To avoid overlap between the mesopelagic and epipelagic community during diel vertical migrations, we exclusively used daytime data, defined here as 2 h before or after sunrise/sunset (Irigoien et al. 2014). Daily sunrise and sunset times were calculated using the {suncalc} package (Thieurmel and Elmarhraoui 2022) in R (R Core Team 2023) with Rstudio (RStudio Team 2023). Data collected when ship speeds fell below 5 knots were excluded to avoid noise. We define the mesopelagic zone as the portion of the water column between 175 and 675 m, over bottom depths ≥725 m. The upper limit (175 m) was selected to omit weak fluid filled epipelagic scatters resonant at depths above 175 m (Davison et al. 2015a) and to coincide with daytime mesopelagic fish depths in the CCE (Davison et al. 2015a). The maximum depth (675 m) corresponds to 50 m above the minimum bottom depth of 725 m and incorporated the vast majority of backscatter from the main scattering layer (Fig. 2), which was the focus of this study. In the CCE, there is occasionally a weaker, deeper scattering layer present below the main DSL, which we did not likely include, as the main scattering layer in our region is consistently above 600 m (Urmy et al. 2012, Davison et al. 2015a, Netburn and Koslow 2015).

### Acoustic data processing

All data filtering and cleaning was conducted using Echoview (Echoview® version 10, 2022). The seabed was distinguished via best bottom candidate algorithms in Echoview or via 18 kHz automatic bottom detection when available (2016–2018) and were visually inspected for accuracy and manually edited where necessary. Acoustic backscatter between 0 and 10 m and within 10 m of the seabed were removed to avoid nearfield effects and interference caused by bottom topography, respectively. In regions of variable, complex bathymetry, such as steep canyons, we additionally removed bottom-associated noise (likely caused by side-lobe interference) extending beyond 10 m above the seafloor. To correct for the effect of variable oceanographic conditions on sound speed and sound absorption, we calculated daily sound speed profiles [using the {oce} package (Richards 2022) "UNESCO" equation of (Fotonoff and Millard (1983)], and absorption coefficient values [calculated in Echoview using the Francois

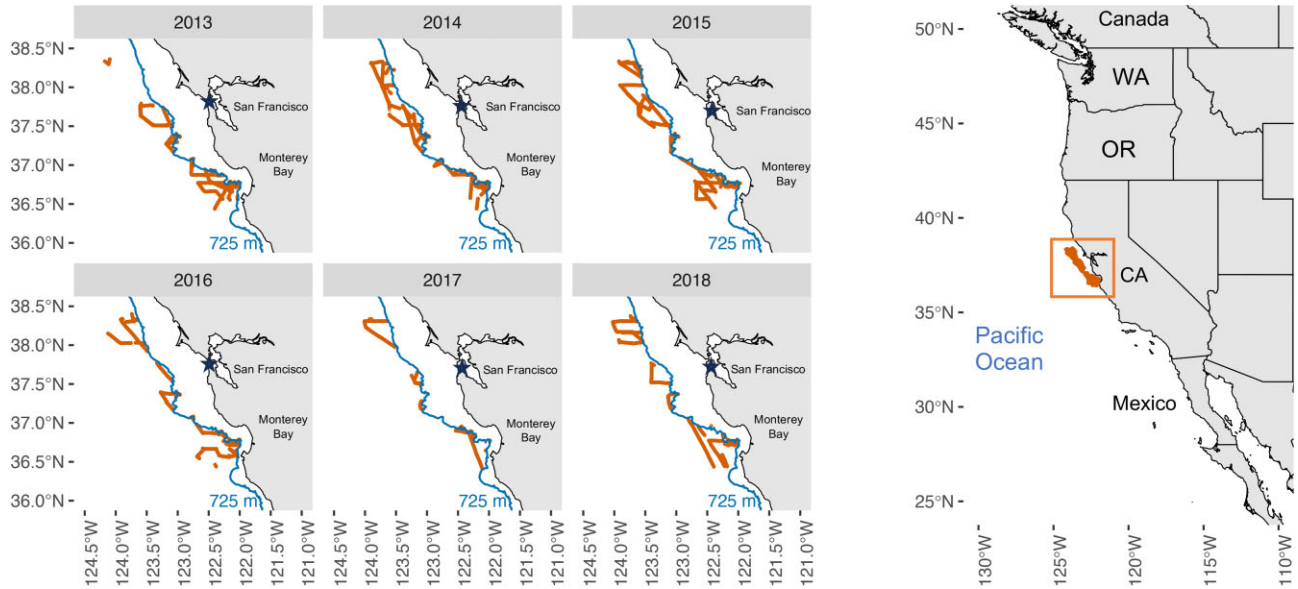


**Figure 1.** The spatial extent of processed acoustics data collected as part of the NOAA RREAS. We selected daytime acoustics data collected from waters with bottom depths deeper than 725 m, and ship speed greater than 5 knots.

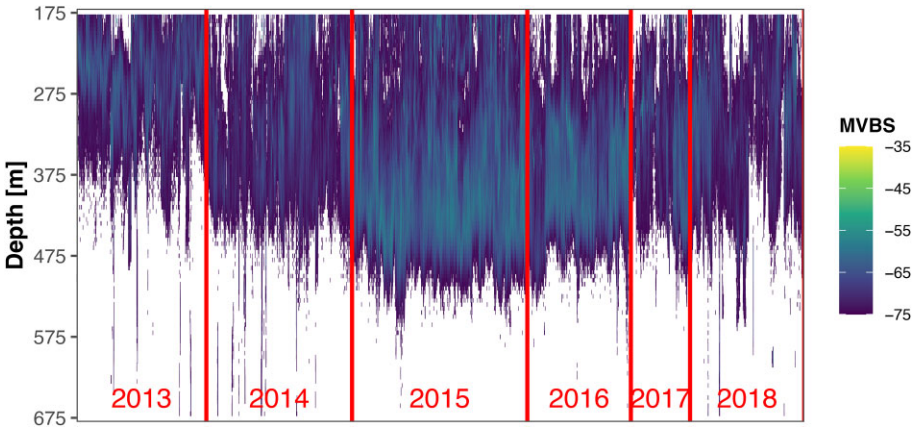


**Figure 2.** Acoustic backscatter measured as mean volume backscattering strength [MVBS, Sv (dB re 1 $m^{-1}$)] for the period from 2013 to 2018. These data have been cleaned and averaged into 100 m horizontal by 5 m vertical bins.

and Garrison (1982) equation], from available CTD measurements of salinity, temperature, and pressure, typically from 2 to 500 m. As pH information was not available from *in situ* measurements, we used the default value of 8.0 as a reasonable approximation for absorption coefficient calculations (Foote et al. 1987). False bottom regions were identified using an angular position algorithm developed by Blackwell et al. (2019, preprint: not peer reviewed) and manually removed. Impulse noise and attenuated signal (Ryan et al. 2015), transient noise (Ryan et al. 2015, Jech et al. 2021), and background noise (De Robertis and Higginbottom 2007) were removed using filters in Echoview. We were unable to account for transducer motion, as boat movement data were not collected at a sufficient sampling rate (Dunford 2005, Ryan et al. 2015, Jech et al. 2021). Throughout processing, we referenced settings recommendations from Ryan et al. (2015), MESOPP (2020), and Haris et al. (2021), adjusted to match our specific data. We gridded cleaned acoustic data into 100 m horizontal by 5 m vertical bins (Davison et al. 2015a), and removed cells with greater than 50% of data removed during cleaning. Volume backscattering strength ( $S_v$) estimates were then exported from Echoview for further analysis.

## Acoustic metrics

DSLs are typically comprised of mixed assemblages of small organisms, generally referred to as micronekton (Brodeur and Yamamura 2005), making it difficult to identify individuals acoustically from echosounders mounted on surface vessels. Acoustic backscatter, measured here as mean volume backscattering strength (MVBS; $S_v$ *or MVBS*), is a logarithmic measure of $s_v$ (volume backscattering coefficient) defined as follows:

$$s_v = \sum \sigma_{bs}/V \ , \qquad (1)$$

where $V$ is volume and $\sigma_{bs}$ is the volume backscattering cross-section (Maclennan et al. 2002). Although we do not have reliable *in situ* biological samples necessary make any inferences about biomass, we consider mean volume-backscattering

strength here as a proxy for acoustic density (Urmy et al. 2012).The mean vertical position of mesopelagic fishes was estimated by calculating centre of mass depth (CM), the mean depth of acoustic backscatter, weighted by $s_v$ (Urmy et al. 2012):

$$CM = \frac{\int z\, s_v(z)\, dz}{\int s_v(z)\, dz}, \quad (2)$$

where $z$ is depth and $s_v(z)$ is the backscattering coefficient at depth $z$. CM is only one proxy for tracking DSL depth, and previous studies have identified upper and lower boundaries of the DSL (Netburn and Koslow 2015) or calculated additional metrics such as evenness or aggregation (Urmy et al. 2012). However, given our broad spatial domain and interest in resolving oceanographic processes occurring at the ~25 km scale, we chose CM as a robust metric for characterizing the depth of the majority of backscatter, similar to previous studies (Klevjer et al. 2016).

## Assessment of spatial autocorrelation

Continuous acoustic sampling can result in spatial autocorrelation, violating the assumption of sample independence required for most statistical tests. Spatial autocorrelation was quantified by plotting correlograms for depth-integrated (175–675 m) MVBS (*mean* $S_v$), over distance sampling units (i.e. horizontal grid cell size) of 100 m using the {ncf} package (Bjornstad 2022). To account for variations in vertical coverage, we excluded from the autocorrelation analysis locations with more than 25 (out of 100) missing vertical cells. Moran's $I$ was calculated as a measure of the degree of correlation in $S_v$ between points at increasing horizontal distances (lags). The distance at which data were no longer spatially autocorrelated was estimated as either the distance where $P$-value > .05, or Moran's $I$ reached 0, whichever came first (Fig. 3). Distances were estimated for each year separately, and a mean and median distance calculated across all years (mean: 27 km, median of 24 km). Based on these values and results of a sensitivity analysis (Fig. S1), we selected a grid cell size of 25 km to avoid spatial autocorrelation. Prior to echo-integration, acoustic backscatter data were regridded using the {raster} package (Hijmans 2023) without imposing a minimum number of vertical cells but ensuring adequate coverage by removing any regridded (25 km × 25 km) cells with less than three (100 m) horizontal cells. The 25-km regridding distance is comparable to the Rossby radius of deformation (~20–30 km average for mid-latitudes in the eastern Pacific; Chelton et al. 1998), which is a natural physical length scale for coastal upwelling in the CCE and has been used previously to characterize acoustic backscatter in our region (Santora et al. 2011).

## Mesopelagic echo classification

There is strong evidence suggesting that within the California Current region, 38 kHz acoustic backscatter in the mesopelagic zone is dominated by fishes (Koslow et al. 2011, Davison et al. 2015b). Hence, we exclusively utilized backscatter data collected at 38 kHz and applied a $S_v$ sample threshold of −75 dB to discriminate fishes from fluid-filled scatters. Based on estimated target strengths (TS) measured by Davison et al. (2015a) from the CCE, we chose a TS value from California Smoothtongue (*Leuroglossus stilbius*), a common species of mesopelagic fish in the CCE lacking a swim bladder (−68.2 dB) and added −6 dB to account for fish not centred in the beam (Rudstam et al. 2009). TS was then related to $S_v$ via:

$$S_v = TS + 10\log_{10}(n), \quad (3)$$

where TS was our minimum TS (−74.2 dB) and n represents the minimum target density (1 fish per 1 $m^3$ water) to give a threshold value of approximately ~ −75 dB. This

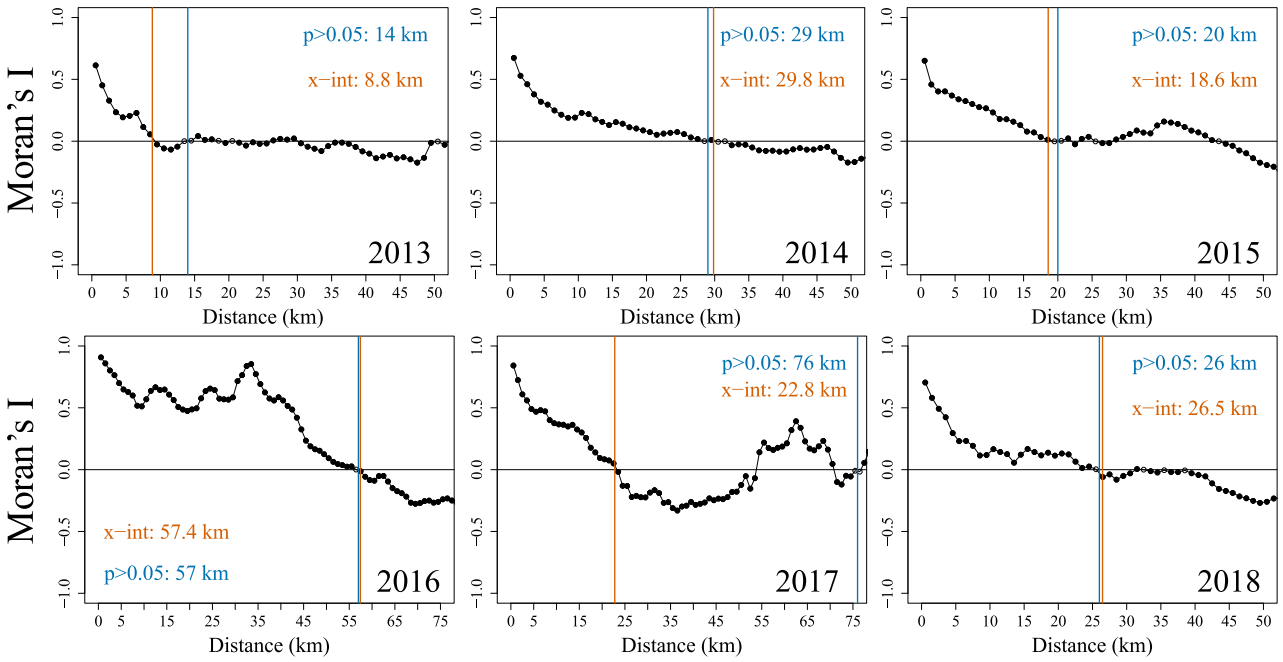


**Figure 3.** Correlograms representing spatial correlation in acoustic backscatter by distance (lag), represented on the *x*-axis. Spatial independence is estimated as either the distance at which Moran's $I = 0$, or the distance at which the *P*-value is no longer significant, whichever distance occurred first. Note that the distance scale for 2016 and 2017 was extended to 75 km.

value falls within the range of threshold values used to distinguish mesopelagic fishes from other forms of backscatter: −90 dB (Irigoien et al. 2014, Klevjer et al. 2016, Aksnes et al. 2017), −65 dB (Escobar-Flores et al. 2019), and −70 dB (Bertrand et al. 1999). We did not have 18 kHz data available in 2013–2015, precluding the use of differential frequency responses to further resolve taxonomic groups (D'Elia et al. 2016). Our analysis may also include backscatter from semipelagic species that aggregate over the shelf-slope boundary, such as Pacific Hake (*Merluccius productus*), which are not considered mesopelagic. We selected acoustic data from bottom depths ≥725 m and integrated to a maximum depth of 675 m to avoid backscatter directly above the bottom and at the shelf break, but this does not guarantee that all benthic/shelf associated fishes were excluded from our analysis. Without direct ground truth data available, our analysis also potentially includes siphonophores with gas inclusions (Davison et al. 2015b, Proud et al. 2019) and dense aggregations of weak-scatters such as zooplankton (Urmy et al. 2012, Davison et al. 2015b, Proud et al. 2019). However, we assume here that the majority of backscatter between 175 and 675 m, with a sample threshold of −75 dB applied, comes from mesopelagic fishes.

## Oceanographic data collection and processing

*In situ* oceanographic data were collected at sea with a calibrated Seabird Electronics SBE9-1050 (2016–2018) and SBE19plus (2013–2015) CTD profiler. Here, we restricted the CTD casts to those that extended to at least 500 m depth and were collected within the acoustic sampling region (Fig. 4). Oceanographic data from the down cast were averaged into 2 m depth bins during postprocessing (Santora et al. 2012). Temperature and salinity measurements were used to calculate density and derive a corresponding dynamic height referenced to 500 m depth. The quality of each cast was further verified by plotting oceanographic variables as a function of depth and visually inspecting individual profiles to remove portions of two casts where salinity and density were well outside their expected range, likely due to instrument error.

For each 25 km × 25 km grid cell containing acoustic data, we extracted available CTD data for temperature, density, and dissolved oxygen at the following depths: 175 m (the upper edge of our mesopelagic region) and 500 m (the deepest CTD data available). Chlorophyll-*a* values were first smoothed using a running mean based on two adjacent 2-m depth bins to account for instrument variability, and then integrated over the upper 100 m of the water column. Dynamic height anomalies were calculated by subtracting the mean dynamic height at 500 m for all CTD casts in our study. We removed two dynamic height values that were greater than three standard deviations from the mean. When more than one CTD cast was available per grid cell, we calculated a mean value from all casts within that cell for a given survey year. If CTD data was unavailable for an acoustic cell, we omitted that cell from analysis, which reduced the overall number of cells from 122 containing acoustic data to 86 that included acoustic data and all oceanographic variables. Since *in situ* light estimates from a PAR sensor were only available for three of the six study years due to a malfunctioning sensor, satellite derived diffuse attenuation coefficients at 490 nm from Aqua MODIS were used as a proxy for light. We chose science quality, 8-day composite data at a resolution of 4 km, as daily composite data had gaps caused by variable cloud cover. Using the {rerddap} (Chamberlain 2023) and {erddapXtracto} (Mendelssohn

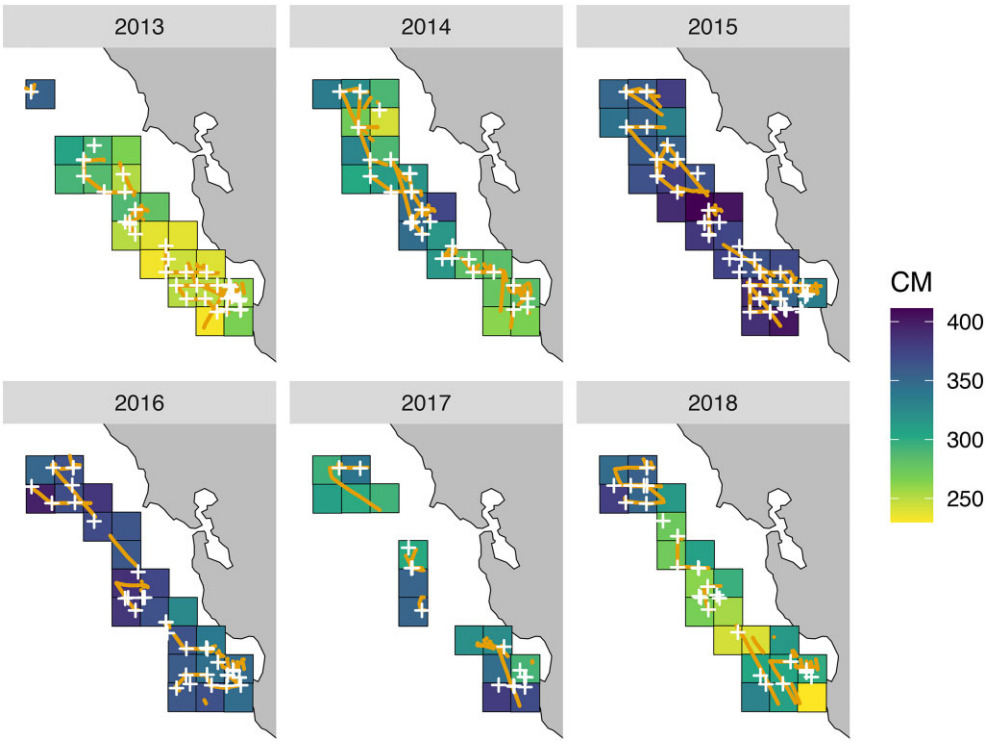


**Figure 4.** 25 km × 25 km grid cells containing both acoustics data and all oceanographic variables. Cells are colored by the mean center of mass depth (m) of mesopelagic fishes estimated from acoustic backscatter, and the white pluses represent the location of oceanographic sampling abord the Rockfish Recruitment and Ecosystem Assessment.

2022) packages, we extracted diffuse attenuation coefficients for the closest 8-day composite data in space and time to our acoustic tracks. The depth at which light reached 1% of surface irradiance ($Z$), which we refer to hereafter as euphotic depth, was calculated as follows:

$$Z = \frac{-\ln\left(E_z/E_o\right)}{K490}, \quad (4)$$

where $E_z$ is irradiance at depth $Z$, $E_o$is the irradiance at the surface, and the 1% light level is given by $E_z/E_o = 0.01$. $Z$ values were then averaged to obtain a mean value per 25 km grid cell.

## Statistical analysis

### Interannual comparison of CM

Differences in CM of mesopelagic fishes between years were examined using a nonparametric Kruskal–Wallis test with a pairwise Wilcox test and Bonferroni correction for multiple comparisons. The Kruskal–Wallis test, selected because of its robustness to the assumptions of normality and variance, uses ranks to tests the null hypothesis that biomass and CM were identical across years. Here, we assume that acoustic estimates of backscatter were independent between years, given the dominant time scales of oceanographic variability in the region and the fluidity of mesopelagic communities between seasons (Urmy et al. 2012). We also conducted a sensitivity analysis comparing our Kruskal–Wallis test results of interannual differences at multiple spatial scales: 1, 5, 10, 15, 20, and 25 km (Fig. S1). Although we were not able to randomize sampling due to the structured nature of the survey, we assume that there was no intentional bias in the acoustic data related to mesopelagic fish.

## Linking CM to environmental covariates

A generalized additive model (GAM) was used to quantify, which environmental covariates explained observed variability in CM. Prior to model fitting, we evaluated collinearity amongst oceanographic covariates and removed those that were highly correlated [correlation coefficient >0.7, as recommended by Dormann et al. (2013)] (Fig. S2). Using the {mgcv} package (Wood 2023), we then fit a GAM with CM as the response variable and temperature (at 175 and 500 m depth), oxygen (at 175 and 500 m depth), chlorophyll-*a* (integrated over 0–100 m depth), dynamic height anomalies, MVBS (as a proxy for acoustic density), and $Z$ (euphotic depth) as environmental covariates. This full model was fit with a Gaussian distribution using the restricted maximum-likelihood method. We used a knots value ($k$) of 10 for the number of basis functions per smooth and verified that this was an appropriate value in {mgcv}. After running the full model, we evaluated pairwise concurvity, a nonlinear measure akin to collinearity that occurs when two smooth terms approximate each other. We removed those terms with "worst" values greater than 0.8. Model fit was evaluated and considered appropriate for our data using both the {mgcv} (Wood 2023) and {gratia} (Simpson 2023) packages (Fig. S3). In addition to MVBS, our final model included temperature and oxygen at 175 m, oxygen at 500 m, chlorophyl integrated over the upper 100 m, dynamic height anomalies, and euphotic depth ($Z$). We chose not to include year or geographic location (latitude and longitude) so that all model variance explained could be attributed to oceanographic variables. While year was not included in our final model, we nevertheless examined variability of oceanographic conditions amongst years to characterize interannual changes in the environment (Fig. S4).

# Results

## Changes in mesopelagic patch size

The spatial autocorrelation analysis indicated strong spatial structuring of the mesopelagic acoustic signal. The distance at which we could assume spatial independence varied among years (Fig. 3), but was twice as great in 2016 as any other year (~57 km in 2016 compared to ~9 km in 2013, 29 km in 2014, 19 km in 2015, 23 km in 2017, and 26 km in 2018). An alternative view of these spatial autocorrelation distances is as the "patch size" of mesopelagic fishes. In this interpretation, 2016 had the largest patch size of mesopelagic fishes ~57 km across. The mean distance of spatial independence across all years was ~27 km, with a median value of ~24 km. The sensitivity analysis, which compared CM across years at multiple horizontal grid resolutions (1, 5, 10, 15, 20, and 25 km), revealed consistent statistical results for interannual centre of mass comparisons for grid cell sizes from 10 to 20 km (see Fig. S1).

## Oceanographic variability

In total, we quantified 3483 km of acoustic data (Table 1) and 191 CTD casts of oceanographic data. The number of CTD casts varied from 13 in 2017 to 51 in 2015 (Fig. 3). Interannual variability of regional upwelling conditions was apparent from our hydrographic sampling before and after the marine heatwave. Specifically, median values of dynamic height anomalies were greatest in 2016 (median of 0.05) and lowest in 2013 (−0.06), indicating stronger upwelling during 2013 and weaker upwelling during 2015, 2016, and 2017 (median: −0.01, 0.05, and −0.01 respectively) (Fig. S4). Euphotic depth, $Z$, inferred from satellite derived diffuse attenuation coefficients (Kd 490) was deepest in 2015 and 2016

**Table 1.** Summary of acoustics data by year. Mean bottom depth below our sampled water column was estimated from {marmap}(Pante and Simon-Bouhet 2013). Dates for acoustic and CTD data represent the range of values included in our analysis from start date to end date.

| Year | Distance sampled (km) | Number of days sampled | Mean bottom depth (m) | Acoustics date range (day/month) | CTD date range (day/month) |
|---|---|---|---|---|---|
| 2013 | 621 | 13 | 1716 | 10/5–1/6 | 10/5–28/5 |
| 2014 | 697 | 18 | 1623 | 3/5–8/6 | 3/5–8/6 |
| 2015 | 839 | 14 | 1899 | 2/5–13/6 | 7/5–14/6 |
| 2016 | 496 | 14 | 1677 | 28/4–3/6 | 27/4–4/6 |
| 2017 | 283 | 10 | 1637 | 28/4–6/6 | 28/4–5/6 |
| 2018 | 546 | 15 | 1803 | 14/5–20/6 | 14/5–20/6 |

(median values of 57.23 m and 54.08, respectively), compared to the shallowest recorded euphotic depth in 2013 (median value of 21.59 m), a difference of ∼30 m (Fig. S4). Median annual temperature at 175 m varied by less than 1°C over our study period, indicating that warming at the surface during the heatwave was not necessarily reflected at mesopelagic depths (Fig. S4). Finally, median dissolved oxygen values appeared to be higher in 2015 and 2016 (2.09 ml/l in 2015 and 2.03 ml/l in 2016) compared to the other years of our study, which ranged from 1.71 ml/l in 2013 to 1.85 ml/l in 2017 (Fig. S4).

### Changes in vertical distribution

The Kruskal–Wallis analysis comparing acoustically estimated CM identified a statistically significant deepening of the median depth of mesopelagic fishes during the marine heatwave (2015 and 2016) compared to other years (Fig. 5). The shallowest CM occurred in 2013 (256 m), a year associated with anomalously strong upwelling conditions and preceding heatwave conditions. The marine heatwave years (2015 and 2016) exhibited significantly deeper centre of mass values (368 m and 364 m) than pre (2013–2014) and post (2017–2018) heatwave conditions and were over 100 m deeper than in 2013. Overall, the CM exhibited a parabolic behavior over our study years (Fig. 5a), starting relatively shallow in 2013, deepening significantly during the marine heatwave (2015–2016), and eventually shoaling following the heatwave, although the CM in 2018 (322 m) had not returned to the shallow levels observed in 2013 (256 m). If we examine these results across the full distribution of CM values (Fig. 5b), 2013 stands apart as having a shallower peak distribution, while 2015 and 2016 exhibit a clear shift to greater deepening and narrowing in the range of centres of mass.

### Environmental drivers of depth distribution

The fitted GAM with oceanographic covariates explained 81.4% of the deviance in CM, reaching model convergence after 12 iterations. Euphotic depth $Z$ (i.e. depth at which light reaches ∼1% of its surface intensity) ($P < .001$, edf: 1.1), dynamic height anomaly ($P < .001$, edf: 3.1), and mean volume backscatter (MVBS) ($P < .001$, edf: 1.9) were all significant covariates explaining variability in CM (Fig. 6). Euphotic depth ($Z$), our proxy for light, exhibited a positive, approximately linear relationship with CM, with CM deepening with increasing light. CM increased (i.e. was deeper) with increasing dynamic height anomalies when dynamic height values were negative (i.e. when there was stronger upwelling, the DSL was shallower). For positive dynamic height values (indicative of weaker upwelling), the CM was stable regardless of additional increases. As acoustic backscatter increased, so did the CM, up to a MVBS value of ∼ −68 dB, at which point the CM levelled-off and even became slightly shallower with further increases. Dissolved oxygen at 175 and 500 m, temperature at 175 m, and chlorophyll-*a* in the upper 100 m did not have a significant effect on CM.

## Discussion

### Connection between near-surface oceanic conditions and mesopelagic communities

Mesopelagic ecosystems are commonly defined by their distance and distinctness from the upper ocean, but our work demonstrates that anomalous and extreme events affecting the upper ocean can impact the vertical daytime distribution of fishes inhabiting mesopelagic depths. During 2015–2016, when a surface intensified marine heatwave impacted the central CCE, the CM of mesopelagic fishes deepened from ∼62 to 112 m and ∼42 to 54 m compared to pre (2013–2014) and post (2017–2018) heatwave conditions. When compared to a strong upwelling year (2013), CM was over 100 m deeper during the heatwave (2015–2016). While most of the warming associated with the marine heatwave was restricted to the upper 50 m of the water column (Zaba and Rudnick 2016, Santora et al. 2017), some heat diffused vertically below the mixed layer where it persisted, even after surface temperatures normalized (Jackson et al. 2018, Scannell et al. 2020). The range of temperatures recorded at 175 m from CTD measurements however, varied by less than 1.2°C across all years (2013–2018) and did not exhibit a marked warming during the heatwave (Fig. S4), indicating that temperature did not increase appreciably at mesopelagic depths during 2015–2016. Vertically migrating mesopelagic fishes were more likely to experience a greater difference in temperatures between 175 and 10 m (on average, ∼3°C–4°C) than the interannual difference at 175 m, which may explain why temperature at 175 m was not a significant covariate in our GAM. Instead, our results suggest that indirect changes in near-surface conditions that impacted the amount of light reaching mesopelagic depths (as measured by euphotic depth, $Z$), was the likely cause of the shift in vertical distribution observed in our study.

The vertical distribution of mesopelagic communities is driven by conflicting needs to feed in productive near-surface waters and to avoid visual predators (Longhurst 1976, Robison et al. 2020). Christiansen et al. (2021) demonstrated that predator interactions increase with increasing light, and when confronted with predators, mesopelagic fishes descend deeper into the water column. Globally, Aksnes et al. (2017) have shown that DSL depth varies across basins based on changes in light penetration, which supports conclusions by Røstad et al. (2016) that there is an optimal light level that mesopelagic communities are selecting for. Light was predicted to exert a greater effect on vertical distribution than temperature in Norwegian Fjords (Langbehn et al. 2019), and mesopelagic communities are even sensitive to short-term changes in light, such as those observed during a passing storm (Kaartvedt et al. 2017). GAM results indicate that light (as approximated in our study by euphotic depth, $Z$) had an approximately linear relationship with CM, with CM increasing with increasing light. This result is consistent with previous work demonstrating that light absorbance can affect the vertical distribution of mesopelagic fishes (Aksnes et al. 2004). The CM of mesopelagic communities in the Gulf of Mexico was likewise associated with light intensity as well as mesoscale oceanographic features (Boswell et al. 2020), indicating that mesopelagic communities respond to changing oceanographic conditions. However, few long-term studies of mesopelagic communities exist, making it difficult to link changing near-surface conditions to changes in mesopelagic communities.

During 2015–2016, upwelling habitat along the central California coast was largely confined nearshore (Santora et al. 2020, Schroeder et al. 2022) and the thermocline and nutricline shifted deeper (Zaba and Rudnick 2016), leading to declines in phytoplankton biomass (Peña et al. 2019). This decrease in phytoplankton biomass, not clearly observed from our CTD measurements, but visible in satellite data over the

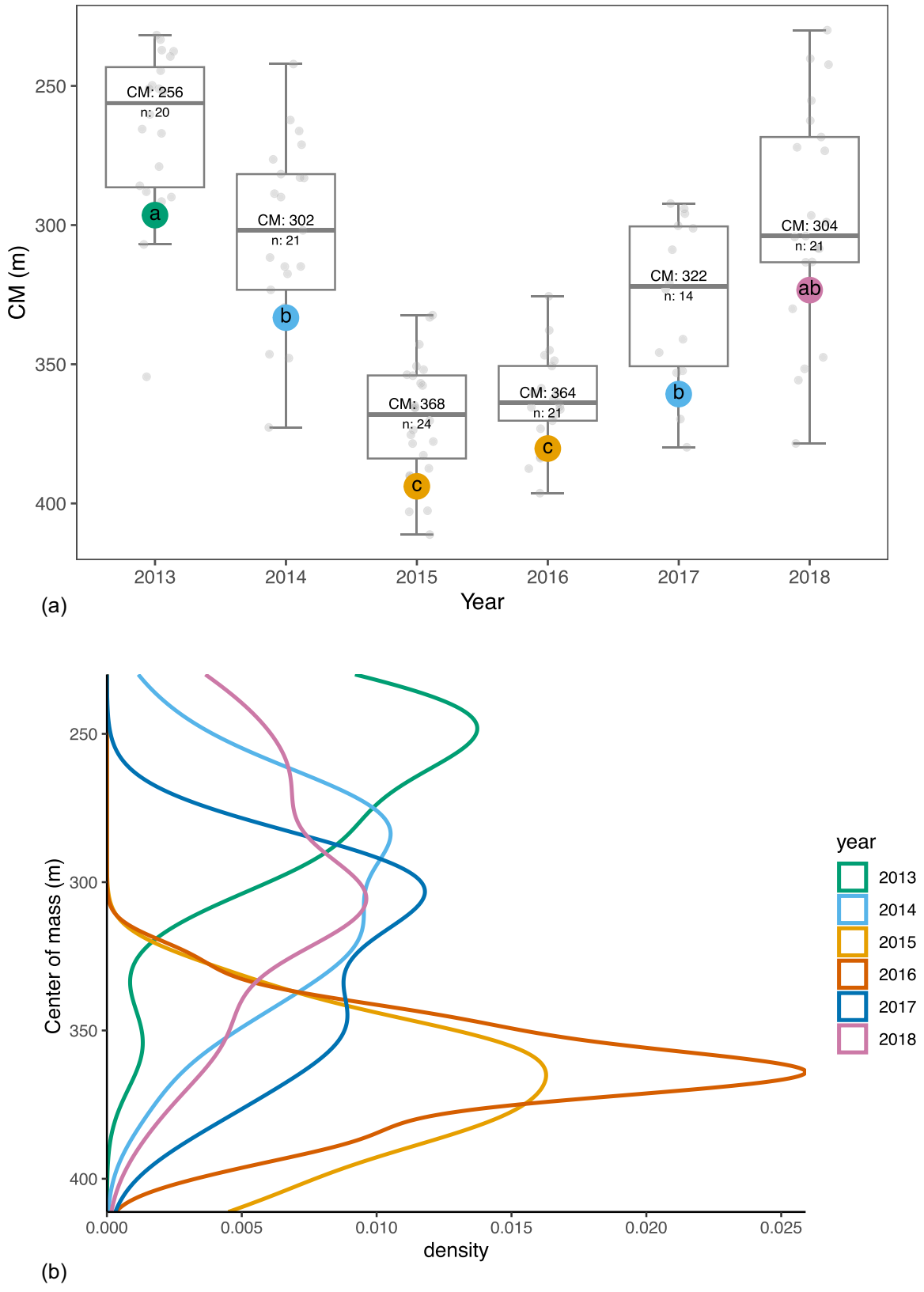


**Figure 5.** Annual estimates of the center of mass depth (m) for mesopelagic fishes estimated from acoustic backscatter. Letters (a, b, c, and ab) denote statistically significant groups determined from Kruskall–Wallis test with multiple comparisons (a) or the distribution of center of mass values between years (b).

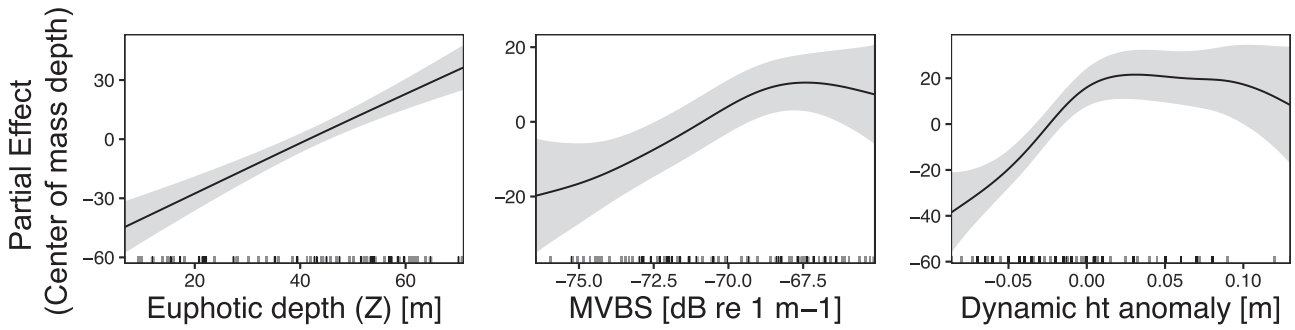


**Figure 6.** GAM plots depicting the partial effect of each significant covariate (*x*-axis) on center of mass depth (*y*-axis). Shaded regions represent confidence bands for smooths 2 standard errors on either side of the smooth, including uncertainty in the global mean.

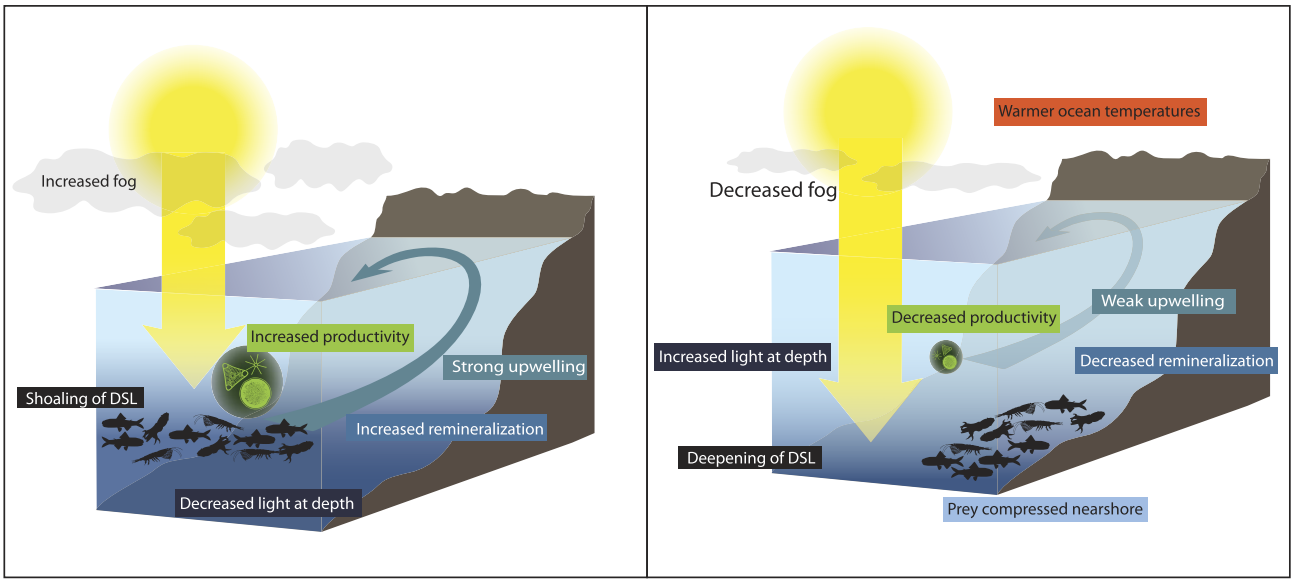


**Figure 7.** A depiction of the mechanism for the observed shift of mesopelagic fishes deeper during the 2015–2016 marine heatwave. A compression of upwelling habitat nearshore during the marine heatwave led to decreases in primary productivity and boundary layer clouds. These factors increased the amount of light that reached mesopelagic depths and mesopelagic fishes responded by shifting deeper into the water column.

extent of our acoustics tracks (Fig. S4), likely allowed more light to penetrate deeper into the water column. We postulate here that mesopelagic fishes responded to this increase in light intensity by moving deeper to evade visual predators (Fig. 7). Evidence for this mechanism comes from our finding that CM was associated with dynamic height anomalies, a proxy for coastal upwelling intensity. Moreover, euphotic depth (Z) was deepest in 2015 and 2016 (over 30 m deeper than in 2013), indicating that the amount of light attenuated by phytoplankton in the water column declined during the heatwave, which allowed for more light to penetrate to mesopelagic depths. Although we did not measure light intensity directly at mesopelagic depths, which limits our ability to make comparisons across ecosystems (Aksnes et al. 2017), our proxy for euphotic depth (Z) derived from Kd490 (8-day diffuse attenuation coefficient at 490 nm from the Aqua MODIS satellite), allowed us to adequately cover the location of our acoustic tracks and infer relative changes in light experienced at mesopelagic depths. In the future, *in situ* measurements of light at mesopelagic depths would allow for more quantitative assessment of the specific light intensities being selected for.

In addition to decreased light attenuation by phytoplankton during the heatwave, there is also evidence supporting a reduction of clouds in the marine layer. Marine layer clouds form as result of differential temperatures between cool, upwelled surface waters, and the atmosphere (Tont 1975). Thus, a reduction of upwelling strength could additionally contribute to increased solar radiation reaching the ocean's surface during the heatwave (Myers et al. 2018, Schmeisser et al. 2019). A combined reduction of phytoplankton biomass and marine layer clouds during the peak of the heatwave for the central California coast in 2015–2016 could thus have led to a compounding effect on light levels at mesopelagic depths. Although light conditions were inferred from 8-day composites of satellite data averaged over 25 km, our results nonetheless provide strong evidence that light intensity in the water column, which increased during the heatwave, affected the vertical distribution of mesopelagic fish. This finding establishes a mechanistic framework for future investigations relating changes in near-surface warming and primary production, to the vertical distribution of mesopelagic fishes, while also highlighting the need to maintain and or establish greater monitoring at mesopelagic depths. Utilization of regional

ocean models to characterize the biophysical conditions of mesopelagic habitats and additional deployments of advanced monitoring technologies such as gliders, cameras, and eDNA may offer an opportunity to fill some of these monitoring needs.

Although we focus here on the vertical distribution of mesopelagic communities, acoustic backscatter (measured as MVBS) was a significant covariate explaining CM and there was a noted increase in MVBS during 2015 and 2016 (Fig. 2 and Fig. S4). This was accompanied by an increase in patch size based on Moran's I, reaching almost 60 km in 2016 (Fig. 3). Although increasing backscatter can, in some cases, indicate increasing biomass (MacLennan and Simmonds 1992), we were not able to distinguish between uncertainties associated with resonance effects (which can increase acoustic backscatter as a function of increasing pressure at depth Godø et al. 2009, Davison et al. 2015a, Kloser et al. 2016, Proud et al. 2019) and changes in the species and length composition of the mesopelagic communities ensonified. For example, some of the most common mesopelagic fishes in the California Current possess gas bladders when young that regress with fat as the fish ages, leading to a counterintuitive decreases in backscatter with increasing size (Davison et al. 2015a). Without knowing the species composition or length distribution of the mesopelagic fish community, we are therefore unable to determine whether changes in acoustic backscatter can be attributed to increasing abundance or changes in the length or species distribution of the mesopelagic community. Of the limited catch data collected concurrently on the RREAS during 2013–2018, there was not an increase in mesopelagic fish during 2015–2016. A likely explanation is that trawling was restricted to the upper water column (between 30 and 45 m), thus inadequately sampling biomass of nonvertically migrating mesopelagic fishes. Furthermore, mesopelagic fishes have patchy distributions in space and time and are often composed of distinct aggregations of individual taxa (Benoit-Bird et al. 2017), the intricacies of which are difficult to capture with discrete trawl samples. Hence, we cannot make definitive conclusions about overall biomass changes during the heatwave relative to other years but recognize that his would be a valuable avenue for future research.

There is, however, some empirical evidence that previous increases in mesopelagic fish abundance in the CCE were linked to warmer ocean temperatures (Thompson et al. 2014, Ralston et al. 2015), as changes in advection likely contributed to a conveyance of oceanic species shoreward (Santora et al. 2017). Some larval mesopelagic fishes with more warm water affinities increased in abundance 3-fold during the heatwave in southern California (Thompson et al. 2022). It is, thus possible that better foraging conditions or warmer temperatures contributed to increased reproductive effort or shifts in the timing of spawning during this time, although it could also indicate changes in the horizontal distribution of mesopelagic taxa during the heatwave. As most of these studies occurred above mesopelagic depths (<200 m), our work also accentuates the need for long-term monitoring programs dedicated to documenting changes in the species composition, abundance, and demographics of mesopelagic communities. Such efforts would help resolve whether changes in acoustic backscatter can be attributed to changes in absolute abundance or related to resonance effects or community demographic changes.

## Broader ecosystem impacts

Mesopelagic fishes are important prey for a diversity of predators within the California Current, including economically valuable and protected species (Iglesias et al. 2023). Recent findings suggest that Albacore foraging within the California Current specifically target shallow mesopelagic scattering layers to reduce energetic costs (Arostegui et al. 2023). During the 2015–2016 marine heatwave, Northern Elephant seals (*Mirounga angustirostris)*, who rely on mesopelagic fishes as critical prey (Goetsch et al. 2018), spent more time foraging at deeper depths (Holser 2023), consistent with our result of a deeper distribution of mesopelagic fishes during this time. Increased vertical movement of both mesopelagic fishes and their predators likely exact a higher energetic cost, but the link between changing distributions of mesopelagic fishes and their higher trophic level predators have been limited by inadequate data on the distribution of mesopelagic prey and incomplete incorporation of mesopelagic taxa in ecosystem-based modeling efforts. Additional research exploring the trophic connections between mesopelagic fish and their higher trophic level predators would allow us to better evaluate and predict the effect of changing ocean conditions on the distribution of top predator populations.

## Mesopelagic communities in an uncertain, but warmer future

Our study demonstrates that mesopelagic fishes inhabiting daytime depths between 175 and 675 m are impacted by surface intensified marine heatwave events. Although this study focuses on a single marine heatwave event in the California Current that peaked in 2015–2016, our findings have broader implications for the impact of changing surface processes on global mesopelagic populations. Proud et al. (2017) predict a mean shoaling of the global mesopelagic zone and an associated increase in the biomass of mesopelagic organisms by 2100. As temperatures continue to warm and the frequency and severity of marine heatwaves is projected to increase (Frölicher et al. 2018), mesopelagic fishes may play an increasingly important role as prey in the broader pelagic ecosystem. Few long-term deep pelagic monitoring programs exist, making it difficult to evaluate the response of mesopelagic fishes to changing ocean conditions. Our multiyear study highlights how using data collected during an ecosystem assessment survey (albeit one not specifically designed to monitor the mesopelagic) can nonetheless inform our understanding of mesopelagic communities and their habitat. A shallower or deeper mesopelagic community could have implications for carbon export and the availability of mesopelagic prey to higher trophic level predators. The interconnectedness of mesopelagic organisms to epipelagic processes provides evidence that mesopelagic ecosystems are susceptible to anthropogenic changes in surface waters and as it pertains to the largest biomass of fishes on Earth, this finding could have cascading effects across both deep pelagic and epipelagic ecosystems.

## Acknowledgements

We would like to thank the officers and crew of the NOAA Ship *Reuben Lasker*, the captain and crew of the R/V *Ocean Starr*, and the many scientists and volunteers who participated in data collection. We would specifically like to thank Keith

Sakuma, chief scientist of the RREAS, for his tireless efforts to collect and maintain survey data, and for his invaluable assistance in accessing archived data. We also thank the Advanced Survey Technologies Group, especially Josiah Renfree at the Fisheries Resources Division of the Southwest Fisheries Science Center for their help in calibrating, maintaining, and troubleshooting the acoustic sensors and systems on these survey vessels. Haley Viehman provided advice on utilizing Echoview software for processing. We thank Tina Fuller Somers for crafting Fig. 7. Finally, we would like to thank Kevin Stierhoff for helpful comments on an earlier draft and our four reviewers, whose feedback and insights improved our manuscript.

## Author contributions

II: conceptualization, formal analysis, funding acquisition, methodology, visualization and writing- original draft preparation JF: conceptualization, funding acquisition, methodology, supervision, writing-review & editing JAS: methodology, validation, visualization, writing-review & editing JCF: conceptualization, funding acquisition, project administration, resources, supervision, writing-review & editing.

## Supplementary data

Supplementary data is available at *ICES Journal of Marine Science* online.

*Conflict of interest*: The authors declare that the research was conducted in the absence of any commercial or financial relationships that could be construed as a potential conflict of interest.

## Funding

This work was partially supported by the Cooperative Institute for Marine, Earth, and Atmospheric Systems (CIMEAS), a partnership between the NOAA Southwest Fisheries Science Center and University of California Santa Cruz (NA20OAR4320278-13). Graduate fellowship funding for I.I. was provided by the University of California, Cota Robles Fellowship and the UC Santa Cruz Chancellor's Dissertation Year Fellowship.

## Data availability

Cleaned acoustics data and hydrographic survey data that support the findings of this study are openly available via Dyrad at https://doi.org/10.5061/dryad.hmgqnk9s0. The R code used to analyse these data are openly available as a Git repository at https://github.com/ilyiglesias/Meso_acoustics (including code for accessing publicly available satellite data).

## References

Aksnes DL, Nejstgaard J, Sædberg E *et al.*. Optical control of fish and zooplankton populations. *Limnol Oceanogr* 2004;**49**:233–8. https://doi.org/10.4319/lo.2004.49.1.0233

Aksnes DL, Røstad A, Kaartvedt S. *et al.* Light penetration structures the deep acoustic scattering layers in the global ocean. *Sci Adv* 2017;**3**:e1602468. https://doi.org/10.1126/sciadv.1602468

Arostegui MC, Muhling B, Culhane E. *et al.* A shallow scattering layer structures the energy seascape of an open ocean predator. *Sci Adv* 2023;**9**:eadi8200. https://doi.org/10.1126/sciadv.adi8200

Benoit-Bird KJ, Au WWL, Wisdom DW. Nocturnal light and lunar cycle effects on diel migration of micronekton. *Limnol Oceanogr* 2009;**54**:1789–800. https://doi.org/10.4319/lo.2009.54.5.1789

Benoit-Bird KJ, Moline MA, Southall BL. Prey in oceanic sound scattering layers organize to get a little help from their friends. *Limnol Oceanogr* 2017;**62**:2788–98. https://doi.org/10.1002/lno.10606

Bertrand A, Le Borgne R, Josse E. Acoustic characterisation of micronekton distribution in French Polynesia. *Mar Ecol Progr Ser* 1999;**191**:127–40. https://doi.org/10.3354/meps191127

Bisson K, McMonagle H, Iglesias I. *et al.* Five reasons to take the precautionary approach to deep sea exploitation. *Commun Earth Environ* 2023;**4**:152. https://doi.org/10.1038/s43247-023-00823-4

Bjornstad ON. ncf: Spatial Covariance Functions. R package version 1.3-2. 2023. https://CRAN.R-project.org/package=ncf.

Blackwell R, Harvey R, Queste B. *et al.* Aliased seabed detection in fisheries acoustic data. 2019. http://arxiv.org/abs/1904.10736

Bond NA, Cronin MF, Freeland H. *et al.* Causes and impacts of the 2014 warm anomaly in the NE Pacific. *Geophys Res Lett* 2015;**42**:3414–20. https://doi.org/10.1002/2015GL063306

Boswell KM, D'Elia M, Johnston MW. *et al.* Oceanographic structure and light levels drive patterns of sound scattering layers in a low-latitude oceanic system. *Front Mar Sci* 2020;**7**:51. https://doi.org/10.3389/fmars.2020.00051

Breitburg D, Levin LA, Oschlies A. *et al.* Declining oxygen in the global ocean and coastal waters. *Science* 2018;**359**:eaam7240. https://doi.org/10.1126/science.aam7240

Brodeur R, Yamamura O. Micronekton of the North Pacific. PICES working group 14 final report. PICES Scientific Report. North Pacific Marine Science Organization (PICES), 2005.

Brodeur RD, Auth TD, Phillips AJ. Major shifts in pelagic micronekton and macrozooplankton community structure in an upwelling ecosystem related to an unprecedented marine heatwave. *Front Mar Sci* 2019;**6**:1–15. https://doi.org/10.3389/fmars.2019.00212

Catul V, Gauns M, Karuppasamy PK. A review on mesopelagic fishes belonging to family Myctophidae. *Rev Fish Biol Fish* 2011;**21**:339–54. https://doi.org/10.1007/s11160-010-9176-4

Cavole L, Demko A, Diner R *et al.*. Biological impacts of the 2013–2015 warm-water anomaly in the Northeast Pacific: winners, losers, and the future. *Oceanography* 2016;**29**:273–85. https://doi.org/10.5670/oceanog.2016.32

Chamberlain S. rerddap: General Purpose Client for 'ERDDAP' Servers_R. R package version 1.0.2. 2023. https://CRAN.R-project.org/package=rerddap.

Chelton DB, deSzoeke RA, Schlax MG *et al.*. Geographical variability of the first baroclinic Rossby radius of deformation. *J Phys Oceanogr* 1998;**28**:433–60. https://doi.org/10.1175/1520-0485(1998)028(0433:GVOTFB)2.0.CO;2

Christiansen S, Klevjer TA, Røstad A *et al.*. Flexible behaviour in a mesopelagic fish (*Maurolicus muelleri*). *ICES J Mar Sci* 2021;**78**:1623–35. https://doi.org/10.1093/icesjms/fsab075

D'Elia M, Warren JD, Rodriguez-Pinto I *et al.*. Diel variation in the vertical distribution of deep-water scattering layers in the Gulf of Mexico. *Deep Sea Res Part I* 2016;**115**:91–102. https://doi.org/10.1016/j.dsr.2016.05.014

Davison P, Lara-Lopez A, Koslow A. Mesopelagic fish biomass in the southern California current ecosystem. *Deep-Sea Res Part II Top Stud Oceanogr* 2015;**112**:129–42. https://doi.org/10.1016/j.dsr2.2014.10.007

Davison PC, Koslow JA, Kloser RJ. Acoustic biomass estimation of mesopelagic fish: backscattering from individuals, populations, and communities. *ICES J Mar Sci* 2015;**72**:1413–24. https://doi.org/10.1093/icesjms/fsv023

De Robertis A, Higginbottom I. A post-processing technique to estimate the signal-to-noise ratio and remove echosounder background noise.

*ICES J Mar Sci* 2007;**64**:1282–91. https://doi.org/10.1093/icesjms/fsm112

Demer DA, Berger L, Bernasconi M *et al.* . Calibration of acoustic instruments. *ICES Cooperative Research Report No 326*. 2015; 133.

Di Lorenzo E, Mantua N. Multi-year persistence of the 2014/15 North Pacific marine heatwave. *Nat Clim Change* 2016;**6**:1042–7. https://doi.org/10.1038/nclimate3082

Dietz RS. The sea's deep scattering layers. *Sci Am* 1962;**207**:44–50. https://doi.org/10.1038/scientificamerican0862-44

Dormann CF, Elith J, Bacher S *et al.*. Collinearity: a review of methods to deal with it and a simulation study evaluating their performance. *Ecography* 2013;**36**:27–46. https://doi.org/10.1111/j.1600-0587.2012.07348.x

Dunford AJ. Correcting echo-integration data for transducer motion. *J Acoust Soc Am* 2005;**118**:2121–3. https://doi.org/10.1121/1.2005927

Escobar-Flores PC, Ladroit Y, O'driscoll RL. Acoustic assessment of the micronekton community on the chatham rise, New Zealand, using a semi-automated approach. *Front Mar Sci* 2019;**6**. 1–22. https://doi.org/10.3389/fmars.2019.00507

FAO. The state of world fisheries and aquaculture. In: *Towards Blue Transformation*. Rome, Italy. 2022. https://doi.org/10.4060/cc0461en

Fennell S, Rose G. Oceanographic influences on deep scattering layers across the North Atlantic. *Deep Sea Res Part I* 2015;**105**:132–41. https://doi.org/10.1016/j.dsr.2015.09.002

Field JC, Miller RR, Santora JA *et al.*. Spatiotemporal patterns of variability in the abundance and distribution of winter-spawned pelagic juvenile rockfish in the California Current. *PLoS One* 2021;**16**:1–25. https://doi.org/10.1371/journal.pone.0251638

Fofonoff NP, Millard RC. Algorithms for the computation of fundamental properties of seawater. UNESCO technical papers in marine science. 1983;**44**:1–53.

Foote KG, Knudsen HP, Vestnes G *et al.*. Calibration of acoustic instruments for fish density estimation: a practical guide. ICES Cooperative Research Report. Copenhagen: ICES, 1987, 1–69.

Francois RE, Garrison GR. Sound absorption based on ocean measurements. Part II: Boric acid contribution and equation for total absorption. *J Acoust Soc Am* 1982;**72**:1879–90. https://doi.org/10.1121/1.388673

Frölicher TL, Fischer EM, Gruber N. Marine heatwaves under global warming. *Nature* 2018;**560**:360–4. https://doi.org/10.1038/s41586-018-0383-9

Gentemann CL, Fewings MR, García-Reyes M. Satellite sea surface temperatures along the West Coast of the United States during the 2014–2016 northeast Pacific marine heat wave. *Geophys Res Lett* 2017;**44**:312–9. https://doi.org/10.1002/2016GL071039

Godø OR, Patel R, Pedersen G. Diel migration and swimbladder resonance of small fish : some implications for analyses of multifrequency echo data. *ICES J Mar Sci* 2009;**66**:1143–8. https://doi.org/10.1093/icesjms/fsp098

Goetsch C, Conners MG, Budge SM *et al.*. Energy-rich mesopelagic fishes revealed as a critical prey resource for a deep-diving predator using quantitative fatty acid signature analysis. *Front Mar Sci* 2018;**5**:1–19. https://doi.org/10.3389/fmars.2018.00430

Haris K, Kloser RJ, Ryan TE *et al.*. Sounding out life in the deep using acoustic data from ships of opportunity. *Sci Data* 2021;**8**:1–23. https://doi.org/10.1038/s41597-020-00785-8

Hijmans R. Raster: Geographic data analysis and modeling. R package version 3.6-20. 2023. https://CRAN.R-project.org/package=raster (11 September 2024, date last accessed).

Holser S. *A Top Predator in Hot Water: Effects of a Marine Heatwave on Foraging and Reproduction in the Northern Elepahnt Seal*. Santa Cruz: University of California, 2023.

Iglesias IS, Santora JA, Fiechter J *et al.* Mesopelagic fishes are important prey for a diversity of predators. *Front Mar Sci* 2023;**10**:1–13. https://doi.org/10.3389/fmars.2023.1220088

IPCC. *Technical Summary: The Ocean and Cryosphere in a Changing Climate: Special Report of the Intergovernmental Panel on Climate Change*. Cambridge: Cambridge University Press. 2019. https://doi.org/10.1017/9781009157964.002(20 November 2023, date last accessed).

Irigoien X, Klevjer TA, Røstad A *et al.*. Large mesopelagic fishes biomass and trophic efficiency in the open ocean. *Nat Commun* 2014;**5**:3271. https://doi.org/10.1038/ncomms4271

Jackson JM, Johnson GC, Dosser HV *et al.*. Warming from recent marine heatwave lingers in deep British Columbia fjord. *Geophys Res Lett* 2018;**45**:9757–64. https://doi.org/10.1029/2018GL078971

Jech JM, Schaber M, Cox M *et al.*. Collecting quality echosounder data in inclement weather. ICES Cooperative Research Report. Copenhagen: ICES, 2021:352.

Kaartvedt S, Røstad A, Aksnes D. Changing weather causes behavioral responses in the lower mesopelagic. *Mar Ecol Progr Ser* 2017;**574**:259–63. https://doi.org/10.3354/meps12185

Kaartvedt S, Staby A, Aksnes D. Efficient trawl avoidance by mesopelagic fishes causes large underestimation of their biomass. *Mar Ecol Progr Ser* 2012;**456**:1–6. https://doi.org/10.3354/meps09785

Klevjer TA, Irigoien X, Røstad A *et al.*. Large scale patterns in vertical distribution and behaviour of mesopelagic scattering layers. *Sci Rep* 2016;**6**:1–11. https://doi.org/10.1038/srep19873

Kloser RJ, Ryan TE, Keith G *et al.*. Deep-scattering layer, gas-bladder density, and size estimates using a two-frequency acoustic and optical probe. *ICES J Mar Sci* 2016;**73**:2037–48. https://doi.org/10.1093/icesjms/fsv257

Koslow JA, Goericke R, Lara-Lopez A *et al.*. Impact of declining intermediate-water oxygen on deepwater fishes in the California Current. *Mar Ecol Progr Ser* 2011;**436**:207–18. https://doi.org/10.3354/meps09270

Langbehn T, Aksnes D, Kaartvedt S *et al.*. Light comfort zone in a mesopelagic fish emerges from adaptive behaviour along a latitudinal gradient. *Mar Ecol Progr Ser* 2019;**623**:161–74. https://doi.org/10.3354/meps13024

Leising AW, Shroeder I, Bograd SJ *et al.*. State of the California current 2014-15: impacts of the warm-water 'blob.'. *CalCOFI Rep* 2015;**56**:31–68.

Liu S, Liu Y, Teschke K *et al.*. Incorporating mesopelagic fish into the evaluation of marine protected areas under climate change scenarios. *Mar Life Sci Technol* 2023;**6**:363–4. https://doi.org/10.1007/s42995-023-00188-9

Longhurst AR. Vertical migration. In: *The Ecology of the Seas*. Philadelphia, Toronto: W.B. Saunders Company, 1976.

Maclennan DN, Fernandes PG, Dalen J. A consistent approach to definitions and symbols in fisheries acoustics. *ICES J Mar Sci* 2002;**59**:365–9. https://doi.org/10.1006/jmsc.2001.1158

MacLennan DN, Simmonds EJ. *Fisheries Acoustics*. London: Chapman and Hall, 1992.

Martin A, Boyd P, Buesseler K *et al.*. Study the twilight zone before it is too late. *Nature* 2020;**580**:26–8. https://doi.org/10.1038/d41586-020-00915-7

Mcclatchie S, Goericke R, Leising A *et al.*. State of the California current 2015-16: comparisons with the 1997-98 El Nino. *CalCOFI Rep* 2016;**57**:1–57.

Mendelssohn R erddapXtracto: Extracts Environmental Data from 'ERDDAP' Web Services. R package version 1.1.4. 2022. https://CRAN.R-project.org/package=rerddapXtracto (11 September 2024, date last accessed).

MESOPP. Report of acoustic processing routines & quality checking methods. Ramonville-Saint-Agne: MESOPP Project Consortium, 2020.

Myers TA, Mechoso CR, Cesana GV *et al.*. Cloud feedback key to marine heatwave off Baja California. *Geophys Res Lett* 2018;**45**:4345–52. https://doi.org/10.1029/2018GL078242

Netburn AN, Koslow AJ. Dissolved oxygen as a constraint on daytime deep scattering layer depth in the southern California Current

ecosystem. *Deep Sea Res Part I* 2015;**104**:149–58. https://doi.org/10.1016/j.dsr.2015.06.006

Nielsen JM, Rogers LA, Brodeur RD *et al.*. Responses of ichthyoplankton assemblages to the recent marine heatwave and previous climate fluctuations in several Northeast Pacific marine ecosystems. *Global Change Biol* 2021;**27**:506–20. https://doi.org/10.1111/gcb.15415

Pante E, Simon-Bouhet B, Irisson J. marmap: Import, Plot and Analyze Bathymetric and Topographic Data. R package version 1.0.10. 2013. https://CRAN.R-project.org/package=marmap (11 September 2024, date last accessed).

Peña M, Olivar MP, Balbín R *et al.*. Acoustic detection of mesopelagic fishes in scattering layers of the Balearic Sea (western Mediterranean). *Can J Fish Aquat Sci* 2014;**71**:1186–97. https://doi.org/10.1139/cjfas-2013-0331

Peña MA, Nemcek N, Robert M. Phytoplankton responses to the 2014–2016 warming anomaly in the northeast subarctic Pacific Ocean. *Limnol Oceanogr* 2019;**64**:515–25. https://doi.org/10.1002/lno.11056

Proud R, Cox MJ, Brierley AS. Biogeography of the Global Ocean's Mesopelagic Zone. *Curr Biol* 2017;**27**:113–9. https://doi.org/10.1016/j.cub.2016.11.003

Proud R, Handegard NO, Kloser RJ *et al.*. From siphonophores to deep scattering layers: uncertainty ranges for the estimation of global mesopelagic fish biomass. *ICES J Mar Sci* 2019;**76**:718–33. https://doi.org/10.1093/icesjms/fsy037

R Core Team. *R: A language and environment for statistical computing*.R Foundation for Statistical Computing, Vienna, Austria. R package version R version 4.2.3 (2023-03-15). 2023. https://www.R-project.org/ (11 September 2024, date last accessed).

Ralston S, Field JC, Sakuma KM. Long-term variation in a central California pelagic forage assemblage. *J Mar Syst* 2015;**146**:26–37. https://doi.org/10.1016/j.jmarsys.2014.06.013

Richards K.. oce: Analysis of Oceanographic Data. R package version 1.7-10. 2022. https://CRAN.R-project.org/package=oce (11 September 2024, date last accessed).

Robison BH, Sherlock RE, Reisenbichler KR *et al.*. Running the gauntlet: assessing the threats to vertical migrators. *Front Mar Sci* 2020;**7**:64. https://doi.org/10.3389/fmars.2020.00064

Røstad A, Kaartvedt S, Aksnes DL. Light comfort zones of mesopelagic acoustic scattering layers in two contrasting optical environments. *Deep Sea Res Part I* 2016;**113**:1–6. https://doi.org/10.1016/j.dsr.2016.02.020

R Studio. Integrated Development Environment for R. Posit Software, PBC, Boston, MA. Version 2023.12.1. 2023. http://www.posit.co/ (11 September 2024, date last accessed).

Rudstam LG, Parker-Stetter SL, Sullivan PJ *et al.*. Towards a standard operating procedure for fishery acoustic surveys in the Laurentian Great Lakes. *ICES J Mar Sci* 2009;**66**:1391–7. https://doi.org/10.1093/icesjms/fsp014

Ryan TE, Downie RA, Kloser RJ *et al.*. Reducing bias due to noise and attenuation in open-ocean echo integration data. *ICES J Mar Sci* 2015;**72**:2482–93. https://doi.org/10.1093/icesjms/fsv121

Sakuma KM, Field JC, Mantua NJ *et al.*. Anomalous epipelagic micronekton assemblage patterns in the neritic waters of the California Current in spring 2015 during a period of extreme ocean conditions. *CalCOFI* 2016;**57**:163–83.

Santora JA, Field JC, Schroeder ID *et al.*. Spatial ecology of krill, micronekton and top predators in the central California Current: implications for defining ecologically important areas. *Prog Oceanogr* 2012;**106**:154–74. https://doi.org/10.1016/j.pocean.2012.08.005

Santora JA, Hazen EL, Schroeder ID *et al.*. Impacts of ocean climate variability on biodiversity of pelagic forage species in an upwelling ecosystem. *Mar Ecol Progr Ser* 2017;**580**:205–20. https://doi.org/10.3354/meps12278

Santora JA, Mantua NJ, Schroeder ID *et al.*. Habitat compression and ecosystem shifts as potential links between marine heatwave and record whale entanglements. *Nat Commun* 2020;**11**:1–12. https://doi.org/10.1038/s41467-019-14215-w

Santora JA, Schroeder ID, Bograd SJ *et al.*. Pelagic biodiversity, ecosystem function, and services. *Oceanography* 2021;**34**:16–37. https://doi.org/10.5670/oceanog.2021.212

Santora JA, Sydeman WJ, Schroeder ID *et al.*. Mesoscale structure and oceanographic determinants of krill hotspots in the California Current: implications for trophic transfer and conservation. *Prog Oceanogr* 2011;**91**:397–409. https://doi.org/10.1016/j.pocean.2011.04.002

Scannell HA, Johnson GC, Thompson L *et al.*. Subsurface evolution and persistence of marine heatwaves in the Northeast Pacific. *Geophys Res Lett* 2020;**47**:e2020GL09054. https://onlinelibrary.wiley.com/doi/10.1029/2020GL090548

Schmeisser L, Bond NA, Siedlecki SA *et al.*. The role of clouds and surface heat fluxes in the maintenance of the 2013–2016 Northeast Pacific marine heatwave. *J Geophys Res Atmos* 2019;**124**:10772–83. https://doi.org/10.1029/2019JD030780

Schroeder ID, Santora JA, Mantua N *et al.*. Habitat compression indices for monitoring ocean conditions and ecosystem impacts within coastal upwelling systems. *Ecol Indic* 2022;**144**:109520. https://doi.org/10.1016/j.ecolind.2022.109520

Simpson G. gratia: Graceful ggplot-Based Graphics and Other Functions for GAMs Fitted using mgcv_. R package version 0.8.1.31. 2023. https://gavinsimpson.github.io/gratia/ (11 September 2024, date last accessed).

Sutton TT, Clark MR, Dunn DC *et al.*. A global biogeographic classification of the mesopelagic zone. *Deep Sea Res Part I* 2017;**126**:85–102. https://doi.org/10.1016/j.dsr.2017.05.006

Thieurmel B, Elmarhraoui A. suncalc: compute sun position, sunlight phases, moon position and lunar phase. R package version 0.5.1. 2022. https://CRAN.R-project.org/package=suncalc (11 September 2024, date last accessed).

Thompson AR, Auth TD, Brodeur RD *et al.*. Dynamics of larval fish assemblages in the California Current System: a comparative study between Oregon and southern California. *Mar Ecol Progr Ser* 2014;**506**:193–212. https://doi.org/10.3354/meps10801

Thompson AR, Ben-Aderet NJ, Bowlin NM *et al.*. Putting the Pacific marine heatwave into perspective: the response of larval fish off southern California to unprecedented warming in 2014–2016 relative to the previous 65 years. *Global Change Biol* 2022;**28**:1766–85. https://doi.org/10.1111/gcb.16010

Tont SA. The effect of upwelling on solar irradiance near the coast of southern California. *J Geophys Res* 1975;**80**:5031–4. https://doi.org/10.1029/JC080i036p05031

Urmy SS, Horne JK, Barbee DH. Measuring the vertical distribution variability of pelagic fauna in Monterey Bay. *ICES J Mar Sci* 2012;**69**:184–96. https://doi.org/10.1093/icesjms/fsr205

Wells BK, Schroeder I, Bograd SJ *et al.*. State of the California Current 2016-17: still anything but 'Normal' in the north. *CalCOFI Rep* 2017;**58**:1–55.

Wood S. mgcv: Mixed GAM Computation Vehicle with Automatic Smoothness Estimation. R Version 1.8-42. 2023. https://doi.org/10.32614/CRAN.package.mgcv (11 September 2024, date last accessed).

Zaba KD, Rudnick DL. The 2014–2015 warming anomaly in the Southern California Current System observed by underwater gliders. *Geophys Res Lett* 2016;**43**:1241–8. https://doi.org/10.1002/2015GL067550

*Handling Editor: Olav Rune Godo*